Regular Paper

Joint Position Estimation for Body Pressure Images during Sleep: An Extension for CPM Using Body Area and Posture Estimation Mashups

Kei Iwase[1,a]   Yu Enokibori[1]   Naoto Yoshida[2]   Kenji Mase[1]

Abstract: Estimating sleeping postures with body joint positions is critical for identifying potential sleeping problems and the risk of pressure ulcers. Many methods have estimated postures with body joint positions from camera images for general purposes. However, visual monitoring of sleeping contexts suffers from privacy and occlusion issues due to blankets, pillows, etc. An approach to solve those issues is the use of body pressure images obtained from bed surfaces. We have developed a textile-based sheet-type pressure sensor to avoid such issues. Unfortunately, its use raises other issues that are absent from camera images such as low resolution and noise caused by the wrinkling of sensor sheets. In this paper, we extend DNN-based joint estimation, called Convolutional Pose Machine (CPM), using body area and posture estimation mashups to improve the accuracy of joint estimation. The following are our evaluation results with cross-validation with 16 joints in six sleeping postures of 12 subjects: 7.15 cm accuracy in mean absolute error (MAE), which is a 33.7% improvement from the standard CPM, and 8.52 cm accuracy in MAE, which is a 37.4% improvement from CPM with camera images in situations using a pillow and a blanket.

Keywords: sleeping posture, body pressure image, joint position estimation, body area estimation, posture classification

1. Introduction

Human sleeping postures can be used as various health indicators. These can be utilized to evaluate not only sleep quality but also estimate the risk of health diseases that occur during sleep, such as pressure ulcers and sleep apnea syndrome. In this paper, we focus on the prevention of pressure ulcers.

One cause of pressure ulcers is that pressure is applied to the same part of the body for many hours. According to an ulcer guidebook [1], seniors and patients with pelvic fractures and spinal cord injuries are at higher risk of pressure ulcers because they find it difficult to change their postures. To prevent pressure ulcers in such bed-ridden patients, changing their postures at roughly two-hour intervals is recommended. Such a burden is onerous on nurses and health-care workers. Since the actual risk differs from patient to patient, depending on body type, weight, sleeping posture, and health conditions, the interval for changing postures can be individually optimized by estimating the risks of the progression of pressure ulcers to reduce nursing burdens.

An e-textile pressure sensor sheet [2], which measures sleeping-body pressure distribution on a bed's surface, consists of an array of capacitive sensor elements constructed by weaving conductive threads. Although sensor sheets visualize the pressure pattern images of sleeping body postures, the images themselves don't provide the relationship to individual body parts where the risks of ulcers is dependent on the body posture. We must identify which part of the body is indicating high pressure. Overlaying body joint positions and a skeleton figure on the images will serve to increase our understanding of the health situations of patients.

Methods for estimating body joint positions from camera images have been actively studied [3], [4], [5], and their estimation accuracy is fairly high. They show good potential for estimating the position of body parts during sleeping. However, such visual monitoring introduces privacy issues and occlusion problems, which are often caused by blankets in a sleeping context. Therefore, we apply a camera-based body joint position estimation method to identify pressure sensor images. However the available pressure image [2] is one-channel and low resolution (80×40 pixels that cover a 160×80 cm area in our case). Thus, the question remains whether such a camera-based method works well even with low-resolution, one-channel images.

We modify the algorithm of the Convolutional Pose Machine (CPM) [4], which is a leading body joint position estimation model, to achieve good estimation of sleeping body posture even with one-channel, low-resolution image data by pressure sensors. We focus on three approaches to modify CPM: (i) noise suppression of sensor data with a body area estimated by U-Net [6] as a mask; (ii) the addition of a classified posture value channel estimated by VGG16 [7]; and (iii) weighting feature vectors in CPM by a classified posture estimated by VGG16 [7]. The contribu-

---

1   Graduate School of Informatics, Nagoya University, Nagoya, Aichi 464–8601, Japan
2   Institute of Innovation for Future Society, Nagoya University, Nagoya, Aichi 464–8601, Japan
a)   iwase@cmc.is.i.nagoya-u.ac.jp

tion of our method is the extension of CPM using these methods ((i)–(iii)) to improve the accuracy of the joint positions estimated from pressure images.

The rest of our paper is organized as follows. Section 2 summarizes related work. Section 3 describes our proposed body joint position estimation method using body area and posture information. Section 4 shows the experimental results and discusses the effect of modifying the estimation accuracy by the proposed method. Section 5 describes the weight parameter investigation for noise suppression. Section 6 concludes the paper.

2. Related Work

Many studies estimate body joint positions and sleeping postures from body pressure. This section describes some of them to clarify the position of our study.

The body joint position estimation method using DNN for camera images is highly accurate. Using a CNN, Toshev et al. proposed a network-based estimation method that predicts end-to-end from feature extraction to describe body joint positions [3]. Wei et al. proposed a method to estimate body joint positions from a wider range of image features by connecting multiple identical network structure CNNs [4]. Cao et al.'s OpenPose system allowed the estimations of body joint positions of multiple people by estimating body joint positions and joint associations using multi-stage CNNs [5]. Since these are camera image-based methods, they are plagued by privacy and occlusion problems.

A method that only estimates sleeping postures using the pressure on beds has also been widely studied. Nishida et al. proposed a system for monitoring respiration and sleeping posture using a pressure sensor with 221 measurement points [8]. Mineharu et al. estimated nine sleeping postures with 77.1% accuracy using a pressure sensor with 32×54 measurement points [9]. Xu et al. estimated six sleeping postures with 90.8% accuracy by a pressure sensor with 64×128 measurement points [10]. Enokibori et al. estimated three sleeping postures with 99.7% accuracy by an optimized deep learning method with an augmented dataset [11].

Recently, both posture classification methods as well as schemes that estimate body joint positions only using pressure have been investigated. Body parts can be identified by estimating body joint positions. This approach can be used to evaluate the body parts at risk of high pressure ulcers. Liu et al. estimated two-dimensional body joint positions in three sleeping postures with an average error of about 3.6 cm. Their method matches the primary parts of a human body [12]. Clever et al. estimated three-dimensional body joint positions in specific sleeping and sitting postures of moving limbs with an error rate of about 7.7 cm. Their method uses CNN and a motion model of human body structures [13]. These studies evaluated joint estimation accuracy using data from the measurements of limited sleeping posture and less pressure noise in experimental environments. To grasp the risks of the progression of pressure ulcers, various sleeping postures must be estimated. In long-term monitoring, pressure noise occurs from dislocated pressure sensors due to the subject changing posture, for example. An estimation method must be robust against pressure noise during long-term monitoring.

We therefore propose a method to improve the accuracy of estimating body joint positions using body area and posture information estimated from sleeping-body pressure images. We verified the accuracy of body joint position estimation in six natural sleeping postures.

3. Body Joint Position Estimation Using Body Area and Posture Information

In this section, we describe a method that features three modifications to the Convolutional Pose Machine (CPM) [4] to improve the accuracy of estimating body joint positions: (i) noise suppression of sensor data using the estimated body area as a mask; (ii) the addition of a classified posture value channel; and (iii) weighting feature vectors in CPM by a classified posture. **Figure 1** shows an overview of the proposed method. In the following, first, we describe CPM, which is the original method we expanded in this study. Next we explain the noise suppression, the addition of a posture channel, and weighting feature vectors.

3.1 Convolutional Pose Machine

CPM is a model that estimates body joint positions and improves accuracy by estimating features in a wider range of images. It connects CNNs with multiple identical structures to extract features and estimate body joint positions. The accuracy is high and the computational cost is small, especially when only one person appears in the image. Since we have just one person per bed, we believe that CPM can estimate body joint positions with high accuracy and a small amount of calculations even from sleeping-body pressure images.

We used such sleeping-body pressure images as input data and such body joint position coordinates as a grand truth, which is generated by semi-manual annotation on color images. We created a model to estimate body joint positions by training these data. A six-stage CPM is employed in our experiment as the base, according to previous research [4]. We supplemented the amount of training data by fine-tuning a model trained in advance with the MPII dataset [14].

3.2 Pressure Noise Suppression with Body Area

The first modification exploits the estimated body area from the input images and uses it as a mask to suppress the sensing noise around the actual body area. **Figure 2** shows an example of (a) an input pressure image, (b) a body area image created manually from its camera RGB image, and (c) a noise suppression result that is masked (a) by (b). The input data (a) is very noisy and noise propagates outward from the bed's areas in contact with the body. Such pressure noise is caused by the wrinkles of the sheet-type pressure sensor, the weight of blankets, humidity offset bias, and so on. We estimate the body area and use it as a mask to reduce the pressure noise outside of the estimated body area, which is estimated from input images by U-Net [6]. U-Net is a convolutional neural network for biomedical image semantic segmentation. Each pixel of the input image is multiplied by different weights: 1.0 for inside the body area and 0.2 for outside it. Thus, noise is suppressed, as shown in Fig. 2 (c). Why the weight for outside of the body area is 0.2 is that the accuracy of estimating body areas by U-Net is not perfect and also there is
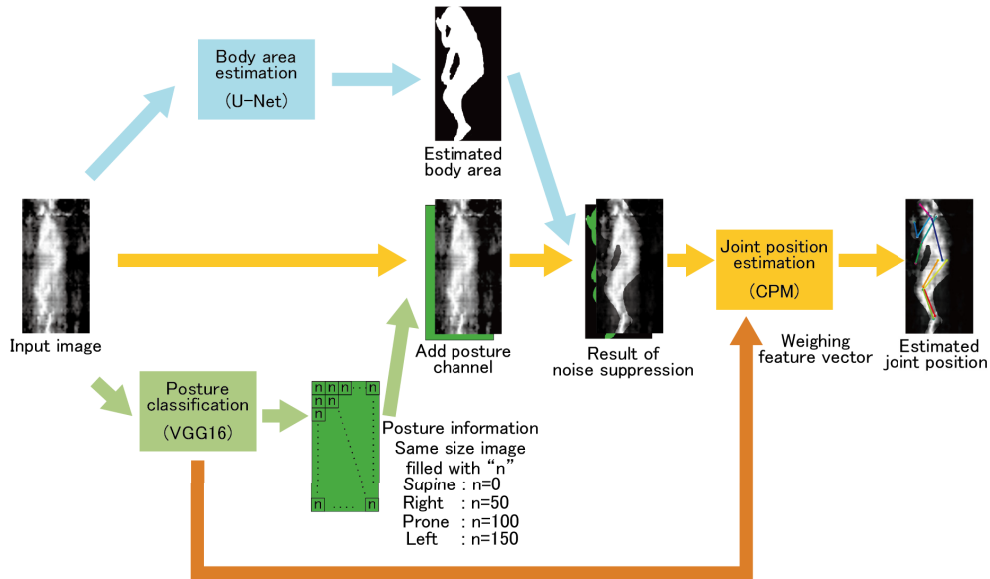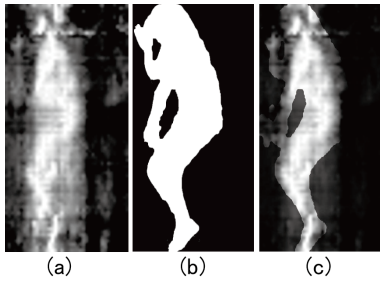
Fig. 1 Overview of proposed method.

Fig. 2 Relationship between pressure data and body area masking for noise suppression: (a) is an input pressure image of sleeping posture, (b) is a body area image created manually from its camera RGB image, (c) a noise suppression result that is (a) masked by (b).

Fig. 3 Feature weighting using posture information.

Fig. 4 Overview of the CPM structure extended with feature weighting structure (modified "Fig. 2" of Ref. [4]).

the possibility that the pressure appeared in out of the body area make some contributions for body joint estimation.

3.3 Original Image Expansion Using Posture Information

The second modification exploits the body posture classification result. The posture class information is embedded as an additional channel of the image. In this case, for an RGB color code image structure, we put the pressure data into the R (red) channel and the posture class label into the G channel, leaving the B channel blank (zeros). By combining all the channels together in CNN, classified posture information can be added to the original pressure image. Large deviations in the estimated joint positions can be reduced by gathering correct information on the sleeping posture types which can be classified into four types from input images by VGG16 [7] (an image-classifying model): supine, right lateral, left lateral, and prone. We fill the posture information channel with different values depending on the types of classified postures: 0 for supine, 50 for right lateral, 150 for left lateral, and 100 for prone. Of course, we had tried to select the values for each posture within DNN automatically. However, this attempt did not demonstrate better performance than that obtained from fixed values. We therefore used fixed values in this study.
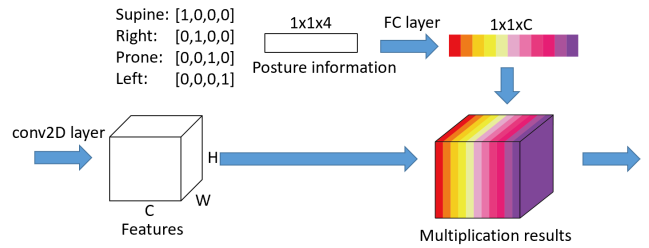
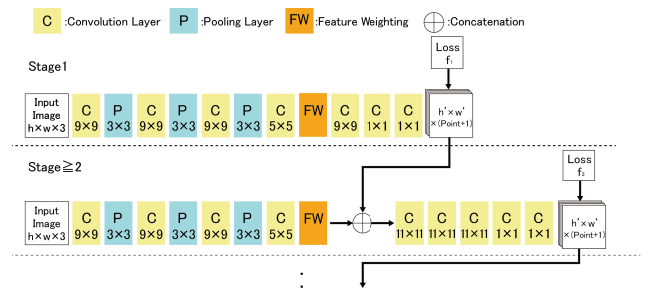### 3.4 Feature Weighting Using Posture Information

The third modification is the weighting for the features in CPM based on the four types of posture classes with structures similar to SENet [15]. **Figure 3** shows how to weight the features by posture classes. We call this extension, "Feature Weight (FW)" block. FW block has two inputs. One input is the output of the previous layer. The another input is the classified posture information which is represented in four-dimensional vectors, i.e., [1,0,0,0] for supine, [0,1,0,0] for the right lateral, [0,0,1,0] for the prone, and [0,0,0,1] for the left lateral. The input classified posture information vector is expanded to the same size of the output of the previous layer through a full connected layer. The FW block generates its output by multiplying the expanded vector by the output from the previous layer. This method makes it possible to select and emphasize the features that are important for each type of posture from the features of the sleeping-body pressure

image in CPM.

Figure 4 shows an overview of the CPM structure and feature weighting structure extension. This figure is a modified image of the "Fig. 2" of [4]. We added the structure of feature weighting after the fourth convolution layers in each CPM stage.

4. Body Joint Position Estimation Experiment

In this section, we experimentally verified the effect of our proposed modifications: noise suppression, addition of a posture channel, and weighting feature vectors. Section 4.1 describes the dataset used for the experiment. Section 4.2 presents the evaluation method including the condition and data set-up and evaluation criterion. Section 4.3 shows the result of improving the estimation accuracy by the proposed method. Section 4.4 discusses the effects of its accuracy improvements based on the results.

4.1 Dataset

To evaluate the accuracy of estimating the body joint positions, we collected the pressure from the sleeping postures, the correct joint positions, the body areas, and the classification posture labels. In this section, we describe the measurement and creation method.

4.1.1 Measurement Environment

To measure the sleeping-body pressure, we used a sheet-type pressure sensor that was covered with a moisture-proof cover and laid it on the mattress. We covered it with box-type sheets. Subjects assumed a sleeping posture and the pressure that was applied to the sheet surface was measured. In addition, a pillow and a blanket were used during the measurement to create an environment closer to that of actual beds. **Figure 5** shows an overview of the measurement. We used the same sheet-type pressure sensor as a previous study [11]. This sensor had 3,200 measurement points (40×80), and the sampling rate was set to about 6 Hz. The sensor was about 90×180 cm, the pillow was about $43 \times 63 \times 10$ cm, and weight 660 g, and the blanket was about $150 \times 210 \times 3$ cm, 1,070 g. To obtain correct joint positions and the body areas of subjects, we captured the sleeping postures with a camera set about 2,350 mm above the sheets (Fig. 5). The camera was set at $1,920 \times 1,080$ for the pixels and 60 Hz for the FPS.

4.1.2 Data Measurement Procedure

In this measurement, our subjects were 12 healthy male university students (S1 to S12) with the following attributes: age, 22.6 ± 1.5 years; height, 172.2 ± 6.6 cm; weight, 64.2 ± 11.0 kg. We

2350mm

Pole

Pillow Blanket Mattress ＋ Sheet−type pressure sensor
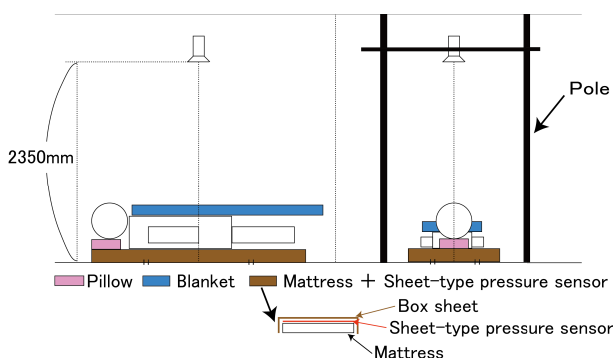Box sheet
Sheet−type pressure sensor
Mattress

Fig. 5 Overview of measurement.

measured the following six sleeping postures (**Fig. 6**): 1 supine (i), 2 right lateral decubituses (ii) and (iii), 1 prone (iv), and 2 left lateral decubituses (v) and (vi). Although the subjects did not lie in exactly identical postures, they assumed natural sleeping postures based on six reference postures we showed them (Fig. 6). Sleeping-body pressure was measured under four conditions: with a pillow and a blanket; with neither a pillow nor a blanket; with a blanket and without a pillow; with a pillow and without a blanket. The subjects changed their sleeping postures according to the experimenter's instructions (we prepared beforehand). The order satisfied all the before/after patterns for combinations of postures from (i) to (vi) in Fig. 6. After changing their posture, the subjects maintained their sleeping posture for five seconds. After that, the experimenter placed the blanket over the subjects and instructed them to maintain the same posture again for five seconds. The data collecting task can be summarized as shown below.

```
foreach (with the pillow and without the pillow):
  for 12 subjects:
    for 12 times:
      for 6 postures:
        -get one data from one 5-second
         posture keeping without the blanket
        -then get one data from one 5-second
         posture keeping with the blanket
```

4.1.3 Post-processing of Body Pressure Data

The measured body pressure data was resampled at 2 Hz and smoothed in the time-series direction. To remove the pressure fluctuation by changing the sleeping postures, we selected a pressure image four seconds after the subjects started to maintain the posture and four seconds after the blanket was placed over them as the sleeping-body pressure image for each posture. We resized the measured sleeping pressure images of 40×80 points into 400×800 points by Bicubic interpolation, which is a curvilinear interpolation method using a weighting function. In addition, we added data inverted along the long axis direction of the sheet to expand the amount of data.

4.1.4 Posture Data Generation

In this section, we explain how to obtain the ground truth of the joint positions, the body areas, and the posture labels.

We estimated the following 16 body joints using OpenPose [5] from the images taken by the camera (**Fig. 7**); 0: r-ankle, 1: r-knee, 2: r-hip, 3: l-hip, 4: l-knee, 5: l-ankle, 6: pelvis, 7: thorax, 8: upper neck, 9: head top, 10: r-wrist, 11: r-elbow, 12: r-shoulder, 13: l-shoulder, 14: l-elbow, and 15: l-wrist. We used the code and trained model in Ref. [16]. To select camera images that correspond to each sleeping body pressure image, we estimated with 30 frames from 3.75 to 4.25 seconds after the subject started to maintain the posture. For each estimated joint point,
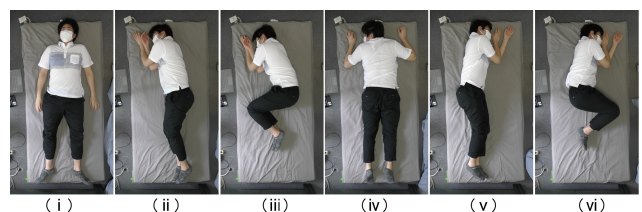

（ⅰ）   （ⅱ）   （ⅲ）   （ⅳ）   （ⅴ）   （ⅵ）

Fig. 6 Reference measurement postures.

Fig. 7   Estimated joint position.

Table 1   Comparison condition.

Pattern	NS	CA	FW
P_{000}^{NCF}	OFF	OFF	OFF
P_{100}^{NCF}	ON	OFF	OFF
P_{010}^{NCF}	OFF	ON	OFF
P_{001}^{NCF}	OFF	OFF	ON
P_{110}^{NCF}	ON	ON	OFF
P_{101}^{NCF}	ON	OFF	ON
P_{011}^{NCF}	OFF	ON	ON
P_{111}^{NCF}	ON	ON	ON

Table 2   Data selection method.

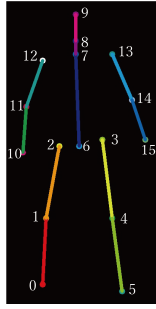| Pattern	Training data	Validation data	Test data
D_{t12}^{v11}	S1–S10	S11	S12
D_{t11}^{v10}	S1–S9, S12	S10	S11
D_{t10}^{v9}	S1–S8, S11, S12	S9	S10
D_{t9}^{v8}	S1–S7, S10–S12	S8	S9
D_{t8}^{v7}	S1–S6, S9–S12	S7	S8
D_{t7}^{v6}	S1–S5, S8–S12	S6	S7
D_{t6}^{v5}	S1–S4, S7–S12	S5	S6
D_{t5}^{v4}	S1–S3, S6–S12	S4	S5
D_{t4}^{v3}	S1, S2, S5–S12	S3	S4
D_{t3}^{v2}	S1, S4–S12	S2	S3
D_{t2}^{v1}	S3–S12	S1	S2
D_{t1}^{v12}	S2–S11	S12	S1

only those whose reliability exceeded 0.3 were averaged and used as joint positions for one posture. If the body joint points could not be estimated, we obtained them manually. Each position was converted into a 400×800 pixel image.

Body areas for the U-Net training were manually created from camera images four seconds after they started to keep the posture for each posture.

Posture labels for the VGG training were created according to the instruction to change postures shown in Section 4.1.2. The types of sleeping posture labels were follows: supine, right, left, or prone.

Finally, we added the inverted body joint positions and body areas created in the same way as the inverted body pressure data and appropriate posture labels. The ground truths of the joint positions, body areas, and posture labels with the blanket were identical as those without the blanket. We made two correct datasets (with and without a pillow) that consisted of 1,728 data.

We made 4 kinds of datasets as follows and each consisting of 1,728 data. We utilized a total of 6,912 data in this experiment.

- without the pillow and the blanket
- without the pillow but with the blanket
- with the pillow but without the blanket
- with the pillow and the blanket

4.2 Accuracy Evaluation Method

In this section, we describe our method that evaluated the accuracy of the estimations of the body joint positions by the proposed method. The model that estimated the body joint positions was trained and evaluated under eight conditions, which are combinations of using/not using each proposed three method: noise suppression (NS) using the body area in Section 3.2, channel addition (CA) using the classified posture information in Section 3.3, and feature weighing (FW) using classified posture information in Section 3.4. **Table 1** shows the eight conditions. Each condition is written as P_{100}^{NCF}. For example, P_{100}^{NCF} means the condition of NS: ON(1), CA: OFF(0), FW: OFF(0). We divided the data for each subject and used them for the evaluations. **Table 2** shows how the data were selected. The training data consisted of the data of ten subjects, the validation data consisted of the data of another subject, and the test data consisted of the data of the remaining subject. All the data select patterns are written in a format given as D_{t12}^{v11}. Here S11 denotes the validation data, S12 is the test data and the remainder is the training data.

U-Net, which is a semantic segmentation model used for the noise suppression, and VGG16, which is a posture classification

model used for the original image expansion and the weighting features, were trained following the data selection method from D_{t12}^{v11} to D_{t1}^{v12}. When estimating the joint positions, we used the estimated results from these models. The accuracy of the body area estimation by U-Net was 0.894 ± 0.017 in the correct pixel ratio, and the accuracy of the posture classification by VGG16 was 0.978 ± 0.022 in the classification success ratio, evaluated based on the data selection method from D_{t12}^{v11} to D_{t1}^{v12}.

As evaluation indexes for estimating the body point positions, we used the mean absolute error (MAE) and the percentage of correct key-points (PCK). The smaller MAE is, the higher the accuracy. The larger PCK is, the higher the accuracy. Although PCK is less affected by outliers than MAE, it is unsuitable for capturing subtle improvements in accuracy. We calculated PCK with every ten pixels of allowable error from 10 to 100 pixels on 400×800 pixel pressure images and used its Area Under the Curve (AUC) as an evaluation index. In this experiment, the error is about 0.2 cm per pixel, so we evaluated PCK every 2 cm from 2 cm to 20 cm. Below, this index is called PCK-AUC@2-20cm.

4.3 Accuracy Evaluation Result

We trained and evaluated the models that estimated the body joint positions in each condition of Table 1 based on a combination of the data selection methods of Table 2. **Table 3** shows the evaluation results of MAE and PCK-AUC@2-20cm. **Figure 8** shows a box plot of the evaluation results in MAE. **Figure 9** shows parts of the PCK graph which is the source of PCK-AUC@2-20cm.

Table 3   Evaluation result.

Improvement rate: from P_{000}^{NCF}

Pattern	MAE (cm)	Improvement rate	PCK-AUC @2-20cm	Improvement rate
P_{000}^{NCF}	10.78 ± 2.03	-	0.662	-
P_{100}^{NCF}	8.16 ± 1.64	0.243	0.721	0.059
P_{010}^{NCF}	12.94 ± 1.89	−0.200	0.602	−0.060
P_{001}^{NCF}	9.80 ± 1.98	0.091	0.681	0.019
P_{110}^{NCF}	7.23 ± 1.22	0.329	0.743	0.081
P_{101}^{NCF}	7.67 ± 1.33	0.288	0.732	0.070
P_{011}^{NCF}	12.41 ± 2.16	−0.151	0.615	−0.047
P_{111}^{NCF}	**7.15 ± 1.25**	0.337	**0.745**	0.083
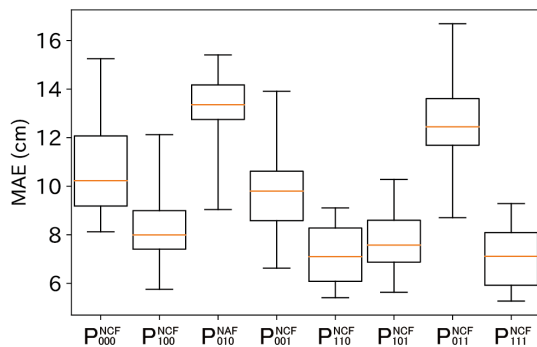
Fig. 8   Evaluation result distribution in MAE.
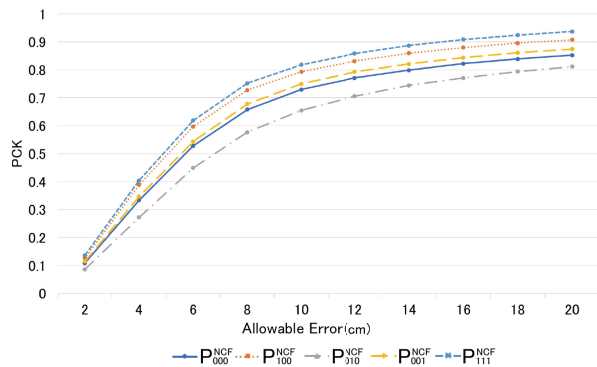
Fig. 9   Evaluation result in PCK.

Next we describe the accuracy improvement effects by each proposed method of noise suppression (NS), channel addition (CA), and feature weighting (FW). As shown in Table 3, the accuracy improved when NS or FW was used compared to CPM alone in both MAE and PCK-AUC@2-20cm. The accuracy dropped significantly when CA was used. When two of the three proposed methods were used, the accuracy improved when NS and CA or when NS and FW were used compared to when each method was used alone. The accuracy improved more when CA and FW were used together than when CA was used alone. The accuracy was lower when FW or no extension was used. The best condition was when all three proposed methods were used together. The accuracy was 7.15 cm in MAE, which is a 33.7% improvement, and 0.745 in PCK, which is an 8.3% improvement, compared to CPM alone. We can estimate the body joint positions with sufficient accuracy to identify the body parts by the proposed method.

For each joint, **Table 4** shows the evaluation result in MAE and

Table 4   Evaluation result of each joint in MAE.

Pattern	r-ankle	r-knee	r-hip	l-hip
P_{000}^{NCF}	15.82 ± 3.63	14.46 ± 4.55	7.24 ± 1.55	7.55 ± 1.69
P_{100}^{NCF}	10.05 ± 3.00	7.45 ± 2.16	6.40 ± 1.45	6.56 ± 1.29
P_{010}^{NCF}	19.14 ± 3.67	18.74 ± 3.72	8.98 ± 1.44	8.96 ± 1.37
P_{001}^{NCF}	14.40 ± 3.86	12.85 ± 4.39	6.96 ± 1.27	7.23 ± 1.39
P_{110}^{NCF}	7.41 ± 1.73	5.71 ± 1.60	**6.02 ± 0.85**	6.14 ± 0.97
P_{101}^{NCF}	9.21 ± 2.72	6.77 ± 1.83	6.22 ± 1.02	6.28 ± 0.99
P_{011}^{NCF}	18.51 ± 4.24	17.51 ± 4.06	8.93 ± 1.65	8.92 ± 1.30
P_{111}^{NCF}	**7.27 ± 1.70**	**5.58 ± 1.51**	**6.02 ± 0.87**	**5.98 ± 0.95**
Pattern	l-knee	l-ankle	pelvis	thorax
P_{000}^{NCF}	14.04 ± 4.03	16.45 ± 3.84	4.83 ± 0.58	4.29 ± 0.87
P_{100}^{NCF}	7.29 ± 2.06	10.10 ± 2.82	4.40 ± 0.61	3.93 ± 0.70
P_{010}^{NCF}	15.74 ± 3.79	18.25 ± 3.71	5.62 ± 0.87	5.05 ± 1.08
P_{001}^{NCF}	12.86 ± 4.22	14.96 ± 3.76	4.87 ± 0.72	4.49 ± 1.02
P_{110}^{NCF}	5.91 ± 1.80	7.19 ± 1.84	**4.24 ± 0.61**	**3.60 ± 0.46**
P_{101}^{NCF}	6.59 ± 1.78	9.13 ± 2.41	4.51 ± 0.81	4.01 ± 0.82
P_{011}^{NCF}	14.64 ± 3.87	17.86 ± 4.05	5.82 ± 1.22	4.91 ± 1.01
P_{111}^{NCF}	**5.85 ± 1.94**	**7.11 ± 1.88**	4.25 ± 0.62	3.62 ± 0.47
Pattern	upper neck	head top	r-wrist	r-elbow
P_{000}^{NCF}	4.95 ± 1.49	5.94 ± 1.56	18.72 ± 3.46	13.55 ± 4.62
P_{100}^{NCF}	4.66 ± 1.23	5.72 ± 1.02	15.48 ± 3.62	9.54 ± 2.76
P_{010}^{NCF}	5.52 ± 1.65	5.98 ± 1.42	21.79 ± 5.02	16.25 ± 4.64
P_{001}^{NCF}	5.14 ± 1.66	6.00 ± 1.69	16.08 ± 3.73	10.80 ± 3.81
P_{110}^{NCF}	**4.24 ± 0.72**	**5.40 ± 0.59**	14.88 ± 3.89	8.98 ± 2.37
P_{101}^{NCF}	4.80 ± 1.34	5.78 ± 1.09	14.47 ± 3.27	8.69 ± 2.24
P_{011}^{NCF}	5.34 ± 1.59	5.96 ± 1.42	20.30 ± 5.52	14.91 ± 4.55
P_{111}^{NCF}	4.29 ± 0.78	5.48 ± 0.61	**14.57 ± 3.94**	**8.77 ± 2.49**
Pattern	r-shoulder	l-shoulder	l-elbow	l-wrist
P_{000}^{NCF}	7.93 ± 2.53	8.14 ± 2.62	11.77 ± 3.36	16.72 ± 3.12
P_{100}^{NCF}	7.43 ± 2.51	7.18 ± 2.46	9.24 ± 2.48	15.2 ± 3.87
P_{010}^{NCF}	9.29 ± 2.26	9.71 ± 2.39	16.06 ± 4.19	21.91 ± 4.58
P_{001}^{NCF}	7.48 ± 2.40	7.45 ± 2.33	10.27 ± 3.12	14.91 ± 3.05
P_{110}^{NCF}	6.61 ± 1.88	6.60 ± 2.10	8.39 ± 2.21	**14.32 ± 3.59**
P_{101}^{NCF}	6.72 ± 2.10	6.74 ± 2.26	8.36 ± 2.07	14.43 ± 3.45
P_{011}^{NCF}	8.91 ± 2.31	9.23 ± 2.31	15.06 ± 4.41	21.78 ± 5.76
P_{111}^{NCF}	**6.53 ± 1.88**	**6.43 ± 2.06**	**8.36 ± 2.35**	14.35 ± 3.73

Table 5 shows it in PCK-AUC@2-20cm. We describe the accuracy improvement effects of each additional proposed method with NS, CA, and FW. When NS was used, the accuracy improved at all the joints in both indexes from CPM alone. When CA was used, the accuracy decreased at all the joints. When FW was used, the accuracy improved at the limbs and decreased at the other joints. When NS and CA were used, or when NS and FW were used, the accuracy improved at all the joints. When CA and FW were used, the accuracy decreased at all the joints. When all three methods were used, eleven joints were the most accurate in both indexes out of sixteen joints. Especially, eleven joints were the most accurate in MAE, and ten joints were the most accurate in PCK-AUC@2-20cm out of twelve joints of the limbs.

Next, we made compared the accuracy under the bedding and

Table 5 Evaluation result of each joint in PCK-AUC@2-20cm.

Pattern	r-ankle	r-knee	r-hip	l-hip
P^{NCF}_{000}	0.524	0.622	0.705	0.692
P^{NCF}_{100}	0.666	0.768	0.751	0.743
P^{NCF}_{010}	0.448	0.512	0.619	0.622
P^{NCF}_{001}	0.563	0.665	0.718	0.705
P^{NCF}_{110}	0.734	0.811	**0.767**	0.760
P^{NCF}_{101}	0.692	0.789	0.757	0.757
P^{NCF}_{011}	0.467	0.541	0.623	0.632
P^{NCF}_{111}	**0.739**	**0.814**	0.766	**0.768**

Pattern	l-knee	l-ankle	pelvis	thorax
P^{NCF}_{000}	0.627	0.515	0.831	0.857
P^{NCF}_{100}	0.770	0.659	0.854	0.876
P^{NCF}_{010}	0.578	0.471	0.788	0.818
P^{NCF}_{001}	0.661	0.550	0.827	0.847
P^{NCF}_{110}	0.806	0.734	**0.861**	**0.892**
P^{NCF}_{101}	0.793	0.686	0.846	0.872
P^{NCF}_{011}	0.597	0.478	0.780	0.826
P^{NCF}_{111}	**0.807**	**0.736**	**0.861**	0.890

Pattern	upper neck	head top	r-wrist	r-elbow
P^{NCF}_{000}	0.826	0.780	0.486	0.614
P^{NCF}_{100}	0.838	0.787	0.513	0.670
P^{NCF}_{010}	0.793	0.773	0.436	0.549
P^{NCF}_{001}	0.813	0.773	0.511	0.663
P^{NCF}_{110}	**0.862**	**0.802**	0.498	0.674
P^{NCF}_{101}	0.831	0.783	0.523	0.685
P^{NCF}_{011}	0.804	0.775	0.455	0.576
P^{NCF}_{111}	0.858	0.798	**0.504**	**0.680**

Pattern	r-shoulder	l-shoulder	l-elbow	l-wrist
P^{NCF}_{000}	0.695	0.684	0.636	0.504
P^{NCF}_{100}	0.718	0.730	0.676	0.517
P^{NCF}_{010}	0.634	0.609	0.540	0.438
P^{NCF}_{001}	0.707	0.706	0.664	**0.525**
P^{NCF}_{110}	0.741	0.745	0.688	0.514
P^{NCF}_{101}	0.742	0.740	0.692	0.525
P^{NCF}_{011}	0.650	0.629	0.561	0.442
P^{NCF}_{111}	**0.747**	**0.753**	**0.689**	0.514

Table 6 Evaluation result between bedding conditions and methods.

Method	Blancket	Pillow	MAE (cm)	PCK-AUC @2-20cm
Ours	OFF	OFF	7.15 ± 1.25	0.745
	ON	OFF	7.56 ± 1.26	0.732
	OFF	ON	8.57 ± 1.34	0.685
	ON	ON	8.52 ± 1.39	0.690
CPM-Camera	OFF	OFF	4.42 ± 1.34	0.874
	ON	ON	13.61 ± 2.22	0.576

With the pillow and the blanket, the accuracy decreased compared to only with the blanket, but it was almost the same compared to only with the pillow.

Next we describe the evaluation results by the proposed method using pressure images or CPM-Camera. Without bedding, the accuracy by CPM-Camera outperformed that of the proposed method. However, with bedding, the proposed method performed better. The accuracy with bedding by the proposed method was 8.52 cm in MAE, which is a 37.4% improvement, and 0.690 in PCK, which is a 11.4% improvement compared to CPM-Camera.

4.4 Discussion

First, we describe the noise suppression using the body areas (NS). In some cases, the pressure of the limbs was confused with noise, and we failed to estimate the limb positions just by using CPM. Then we hypothesize that the estimation accuracy of the limb joints could probably be improved by noise suppression using the body areas. From the evaluation results, the accuracies of all the joints improved, especially the limbs. Therefore, noise suppression by body area effectively improved the accuracy of the joint position estimation.

Second, we describe the channel addition using the classified posture information (CA). When CA was used without NS, the accuracy decreased more than with CPM only. When CA was used with NS, the accuracy improved more than when only NS was used. When only CA was used, the noise seemed to be added to the sleeping-body pressure images. That decreased the estimation accuracy. When CA was used with NS, the effect of noise addition by CA was suppressed, and the accuracy improved by adding posture information.

Third, we describe the feature weighting using the classified posture information (FW). When FW was used, the accuracies improved in all the conditions compared to those without FW. Therefore, feature weighting effectively improved the accuracy. In addition, the accuracy when NS, CA, and FW were used exceeded that when NS and CA were used. Although CA and FW added the same posture information, a synergistic effect was created when they were used together. Perhaps the effect of adding posture information was different between CA and FW.

With our proposed methods, noise suppression, channel addition, and feature weighing, each individually improved the accuracy.

Next we describe the effects from bedding on the accuracy. With the pillow, the accuracy decreased with or without a blan-
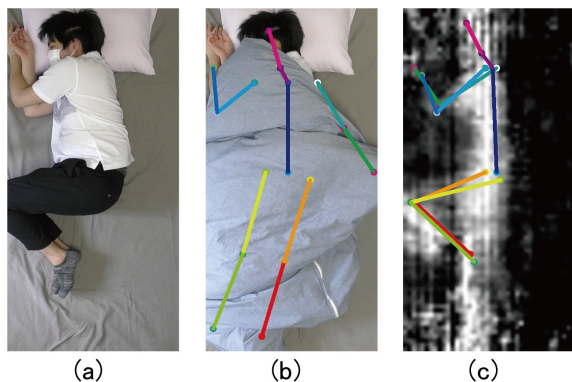
method conditions shown in **Table 6**. We used original CPM as a camera-based scheme. In this experiment, we call the method for estimating body joint positions using original CPM from camera images, the "CPM-Camera" method. Table 6 shows the evaluation results of four types of pressure image datasets with/without the pillow and the blanket by the proposed method, and two types of sleeping posture camera image datasets with/without bedding by CPM-Camera.

First, we describe the evaluation results by the proposed method from the four datasets: with a pillow and a blanket, with neither a pillow nor a blanket, with a blanket and without a pillow, with a pillow and without a blanket. In both the MAE and PCK-AUC@2-20cm indexes, only with the pillow and only with blanket, the accuracy was reduced compared to without bedding.

Fig. 10 Sample: (a) Camera image without blanket, (b) Estimated result by CPM from camera image with blanket, (c) Estimated result by proposed method from pressure image.

ket. The decrease in accuracy was caused by pressure noise near the head and from changes in the pressure that were applied to the bed surface. Without the pillow, the accuracy with the blanket decreased more than without the blanket. On the other hand, with the pillow, the accuracy with the blanket was almost the same as without the blanket. The effect provided by the blanket is smaller than that of the pillow. However, we can estimate the body joint point positions without significantly decreasing the accuracy even when using bedding by the proposed method.

Finally, we describe the result of our proposed method and CPM-Camera. **Figure 10** shows an example of the result of estimating body joint positions with bedding. With the blanket, the joint positions estimated by CPM-Camera were significantly different from the correct position. However, joint positions could be estimated by the proposed method from the pressure images. Our proposed method is useful in actual bed environments with pillows and blankets.

5. Weight Parameter Investigation for Noise Suppression

In this section, we describe the weight parameter investigation for noise suppression. As described in Section 3.2, we used the 0.2 weight for outside of the body area because the accuracy of estimating body areas by U-Net is not perfect and there is also the possibility that the pressure appeared in out of the body area make some contributions for body joint estimation. However, the weight parameter "0.2" was selected manually from a small preliminary trial. We then searched for a suitable weight parameter for our method.

5.1 Investigation Method

We searched for a suitable weight parameter by two method. In this investigation, we used the dataset without the pillow and the blanket shown in Section 4.1, and the model added the three proposed method shown in Section 3. The accuracy evaluation method is the same as that shown in Section 4.2.

First, we investigated weight parameters by setting manually. We checked the results in the case of using the weight parameter every 0.1 from "0" to "0.5" by the whole data and proposed methods.

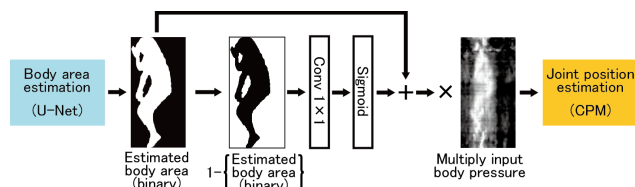Second, we checked the cases of DNN based auto weighting.

Fig. 11 Overview of DNN based auto weighting.

Table 7 Weight parameter investigation result.

Method		MAE (cm)	PCK-AUC @2-20cm
manually selected parameter	0	7.36 ± 1.27	0.744
	0.1	7.13 ± 1.22	0.746
	0.2	7.15 ± 1.25	0.745
	0.3	7.10 ± 1.24	**0.747**
	0.4	**7.07 ± 1.25**	**0.747**
	0.5	7.12 ± 1.26	0.746
DNN based		12.89 ± 2.85	0.576

Figure 11 shows the overview of this method. We added a 1×1 kernel size convolution layer after the U-Net part. The out of person area estimated by U-Net was passed through the convolution layer and then multiplied by the input pressure image. We assumed the weight parameter for noise suppression could be tuned by this layer.

5.2 Investigation Result

We show the result of investigation in **Table 7**. The first method, manual parameter setting, the result of "0" was the worst and that of "0.4" was the best. This result shows that the pressure outside of the body area estimated by U-Net make some contributions to body joint estimation. In the second method using DNN-based auto weighting the accuracy become worse.

In this investigation the "0.4" weight parameter proved best in this study. However, it may prove possible to find a more optimal parameter.

6. Conclusion

We examine a method to estimate body joint positions from sleeping-body pressure images. Our method, which suffers from fewer privacy or occlusion issues, identifies areas where pressure ulcers might be progressing in bed-ridden patients.

We improved the accuracy of estimating the body joint point positions by proposing three approaches to modify CPM: noise suppression using estimated body areas, channel addition using classification posture information, and feature weighting using classification posture information. With these proposed methods, we obtained the following accuracy measurements in estimating body joint positions from sleeping-body pressure images: 7.15 cm in MAE, which is a 33.7% improvement, and 0.745 in PCK, which is an 8.3% improvement compared to CPM alone. Our proposed methods improve the accuracy of joint position estimation.

Future work will expand this method to 3D joint position estimation and apply it to use in actual hospitals and long-term care

facilities.

References

[1] Ariga, H.: *Guidebook for Pressure Ulcers, 2nd edition, Compliant with pressure ulcer prevention and management guidelines (4th edition). in Japanese*, Japanese Society of Pressure Ulcers, Shorinsha Inc. (2015).

[2] Enokibori, Y., Suzuki, A., Mizuno, H., Shimakami, Y. and Mase, K.: E-textile pressure sensor based on conductive fiber and its structure, *UbiComp 2013 Adjunct-Adjunct Publication of the 2013 ACM Conference on Ubiquitous Computing*, pp.207–210 (2013).

[3] Toshev, A. and Szegedy, C.: Deeppose: Human pose estimation via deep neural networks, *IEEE Conference on Computer Vision and Pattern Recognition*, pp.1653–1660 (2014).

[4] Wei, S.-E., Ramakrishna, V., Kanade, T. and Sheikh, Y.: Convolutional pose machines, *IEEE Conference on Computer Vision and Pattern Recognition*, pp.7291–7299 (2017).

[5] Cao, Z., Hidalgo, G., Simon, T. and S. Wei, Y.: Realtime Multi-Person 2D Pose Estimation using Part Affinity Fields, *IEEE Conference on Computer Vision and Pattern Recognition*, pp.7291–7299 (2017).

[6] Ronneberger, O., Fischer, P. and Brox, T.: U-Net: Convolutional Networks for Biomedical Image Segmentation, *Medical Image Computing and Computer-Assisted Intervention (MICCAI)*, Vol.9351, pp.234–241 (2015).

[7] Simonyan, K. and Zisserman, A.: Very Deep Convolutional Networks for Large-Scale Image Recognition, *International Conference for Learning Representations* (2015).

[8] Nishida, Y., Takeda, M., Mori, T., Mizoguchi, H. and Sato, T.: Unrestrained and Non-invasive Monitoring of Human's Respiration and Posture in Sleep Using Pressure Sensors, *Journal of the Robotics Society of Japan*, Vol.16, No.5, pp.705–711 (1998).

[9] Mineharu, A., Kuwahara, N. and Morimoto, K.: A study of automatic classification of sleeping position by a pressure-sensitive sensor, *International Conference on Informatics, Electronics & Vision (ICIEV)*, pp.1–5 (2015).

[10] Xu, X., Lin, F., Wang, A., Song, C., Hu, Y. and Xu, W.: On-bed sleep posture recognition based on body-earth mover's distance, *Biomedical Circuits and Systems Conference (BioCAS 2015)*, pp.1–4 (2015).

[11] Enokibori, Y. and Mase, K.: Data Augmentation to Build High Performance DNN for In-bed Posture Classification, *Journal of Information Processing*, Vol.26, pp.718–727 (2018).

[12] Liu, J.J., Huang, M.-C., Xu, W. and Sarrafzadeh, M.: Bodypart localization for pressure ulcer prevention, *IEEE Engineering in Medicine and Biology*, pp.766–769 (2014).

[13] Clever, H.M., Kapusta, A., Park, D., Erickson, Z., Chitalia, Y. and Kemp, C.C.: Bodies at Rest: 3D Human Pose and Shape Estimation From a Pressure Image Using Synthetic Data, *International Conference on Intelligent Robots and Systems*, pp.54–61 (2018).

[14] Andriluka, M., Pishchulin, L., Gehler, P. and Schiele, B.: 2D human pose estimation: New benchmark and state of the art analysis, *IEEE Conference on Computer Vision and Pattern Recognition*, pp.3686–3693 (2014).

[15] Hu, J., Shen, L., Albanie, S., Sun, G. and Wu, E.: Squeeze-and-Excitation Networks, *IEEE Conference on Computer Vision and Pattern Recognition*, pp.7132–7141 (2018).

[16] CMU-Perceptual-Computing-Lab: GitHub - CMU-Perceptual-Computing-Lab/openpose: OpenPose: Real-time multi-person keypoint detection library for body, face, hands, and foot estimation, available from ⟨https://github.com/CMU-Perceptual-Computing-Lab/openpose⟩ (accessed 2021-04-22).

Kei Iwase received his B.E. degree in Engineering from Nagoya University in 2020. He is a M.I. candidate with Graduate School of Informatics, Nagoya University. His research interest is health care computing. He is a student member of the Information Processing Society of Japan (IPSJ).

Yu Enokibori received his B.E., M.E., and Ph.D. degrees in Engineering Science from Ritsumeikan University in 2005, 2007, and 2010, respectively. He be came an assistant professor at Graduate School of Information Science, Nagoya University in 2015, and an assistant professor at Graduate School of Informatics, Nagoya University in 2017. He is now a lecturer with Graduate School of Informatics, Nagoya University since 2020. His research interests include ubiquitous computing, wearable computing, invisible computing, healthcare and medical computing, and human computer interaction. He is a member of the Information Processing Society of Japan (IPSJ), the Institute of Electronics, Information and Communication Engineers (IEICE), the Japan Society of Artificial Intelligence (JSAI), the Society of Biomechanisms Japan (SOBIM), the Japan Academy of Nursing Science (JANS), and the ACM.

Naoto Yoshida received his Ph.D. degree in Informatics from Kansai University in 2018, respectively. He was a Japan Society for the Promotion of Science (JSPS) Research Fellow at Kansai University in 2017–2019. He is an designated associate professor of the Institute of Innovation for Future Society, Nagoya University. His research interests include multimodal anthropomorphic agent systems, communication robots, cognitive training systems for the elderly, walking support devices, virtual reality system. He is a member of the Information Processing Society of Japan (IPSJ).

Kenji Mase received his B.E. degree in Electrical Engineering and his M.E. and Ph.D. degrees in Information Engineering from Nagoya University in 1979, 1981 and 1992 respectively. He became professor of Nagoya University in August 2002. He is now with the Graduate School of Informatics, Nagoya University. He is Research Supervisor of JST CREST on Symbiotic Interactions since 2017. He joined the Nippon Telegraph and Telephone Corporation (NTT) in 1981 and had been with the NTT Human Interface Laboratories. He was a visiting researcher at the Media Laboratory, MIT in 1988–1989. He had been with ATR (Advanced Telecommunications Research Institute) in 1995–2002. His research interests include multimodal interaction, artificial intelligence and their applications for computer-aided communications, wearable/ubiquitous computers, and e-coaching. He is a Fellow of Institutes of Electronics, Information and Communication Engineers (IEICE) of Japan, and member of the Information Processing Society of Japan (IPSJ), Japan Society of Artificial Intelligence (JSAI) and ACM, and a senior member of IEEE Computer Society. He was Section Chairs of IEEE Nagoya Section in 2014–2015 and IPSJ Tokai Section in 2020–2021. He has been the 24th–25th associate member of Science Council of Japan.